

# The water color simulator WASI: an integrating software tool for analysis and simulation of optical in situ spectra<sup>☆</sup>

Peter Gege\*

*DLR, Remote Sensing Technology Institute, P.O. Box 1116, Wessling 82230, Germany*

Received 11 August 2003; received in revised form 3 March 2004; accepted 12 March 2004

## Abstract

A WINDOWS-based program was developed for modeling and analyzing optical in situ measurements in aquatic environments. It supports eight types of spectra which are commonly measured by instruments on ship: downwelling irradiance above and below the water surface, upwelling radiance above and below the surface, remote sensing reflectance above and below the surface, irradiance reflectance, specular reflectance at the water surface, absorption, attenuation, and bottom reflectance. These spectra can either be simulated (by forward calculation) or analyzed (by inverse modeling) using well-established analytical models. The variability of a spectrum is determined by up to 25 parameters, depending on the spectrum type. All model constants and input spectra can be changed easily for adaptation to a specific region. Effective methods are included for dealing with series of spectra. For some spectrum types, inversion is a critical task and can produce erroneous results, that is when different parameter combinations cause similar spectra. In order to handle this problem, specific inversion techniques are implemented for critical spectrum types, and measures are included which allow fine-tuning of the fit procedure by the user.

© 2004 Elsevier Ltd. All rights reserved.

*Keywords:* Spectral measurements; Water; Analytical models; Inversion

## 1. Introduction

Optical sensors on ship provide many different types of spectra: up- and downwelling radiance above and below the surface, vector and scalar irradiance of the upper and lower hemisphere in air and water, irradiance reflectance, remote sensing reflectance, attenuation, absorption, scattering, backscattering, and others. Usually data from each instrument are analyzed with software that is specifically tailored to that instrument or spectrum type. However, operating a fleet of programs is a potential source of errors, because the data analysis programs must be consistent with each other concerning the model and input data. In addition, maintenance and data handling is time consuming, as is training new staff.

For these reasons it is desirable to have one single integrating software. That was the motivation to develop a comfortable, sensor-independent software tool for forward and inverse calculations of major types of spectra in aquatic environments which can be applied for data analysis, data simulation, sensitivity studies, and student training. The resulting “Water colour Simulator” WASI is described in this article. It is available as an executable program free of charge and can be downloaded together with a user manual (Gege, 2002) from an ftp server.

## 2. Concept

### 2.1. General features

WASI is designed as a sensor-independent spectra generator and spectra analyzer with well-documented calculation steps and automatic result visualization.

<sup>☆</sup> Code and manual available by anonymous ftp from <http://ftp.dfd.dlr.de> in directory /pub/WASI.

\*Fax: +49-8153-28-1444.

E-mail address: [peter.gege@dlr.de](mailto:peter.gege@dlr.de) (P. Gege).

The supported spectrum types are listed in Table 1. Forward calculation as well as inversion is implemented for all types, i.e. all spectra can be simulated and analyzed. The variability of a spectrum is determined by up to 25 parameters, depending on the spectrum type. A complete list of all 36 parameters is given in Table 2.

All input and output files are in text format (ASCII), making it easy to adapt the calculations to regional specifics by replacing some default input spectra and changing material-specific constants. Spectral data interval, number, and position of spectral channels are arbitrary: the spectra can either be calculated for equidistant wavelengths, or for arbitrary spectral channels whose center wavelengths are read from a text file. Spectral weighting within channels using sensor-specific response functions is not supported.

WASI was developed for PC environments using WINDOWS as the operating system. The programming language is Borland Delphi 6. The program consists of the executable file WASI.EXE, an initialization file WASI.INI, and 25 input spectra. The input spectra are listed in Table 3. Several input spectra and model constants may be test-site specific. The data provided with WASI were determined at Lake Constance (Gege, 1994, 1995; Heege, 2000), and are suited for calculating all spectrum types of Table 1 at least from 390 to 800 nm at a spectral resolution of 1 nm.

Table 1  
Spectrum types and major model options

Spectrum type	Model options	Symbol	Equation
Absorption	Exclude pure water	$a_{WC}(\lambda)$	(1)
	Include pure water	$a(\lambda)$	(3)
Attenuation	—	$K_d(\lambda)$	(5)
	Wavelength dependent	$R_{rs}^{surf}(\lambda)$	(8a)
Constant		$R_{rs}^{surf}$	(8b)
Irradiance reflectance	—	$R(\lambda)$	(9)
Remote sensing reflectance	Below surface	$R_{rs}^{-}(\lambda)$	(11)
	Above surface	$R_{rs}(\lambda)$	(12)
Bottom reflectance	For irradiance sensors	$R^b(\lambda)$	(13)
	For radiance sensors	$R_{rs}^b(\lambda)$	(14)
Downwelling irradiance	Above surface	$E_d(\lambda)$	(15)
	Below surface	$E_d^{-}(\lambda)$	(16)
Upwelling radiance	Below surface	$L_u^{-}(\lambda)$	(18)
	Above surface	$L_u(\lambda)$	(19)

## 2.2. The file WASI.INI

All program settings are stored in ASCII format in a single file, WASI.INI. It contains the file names of the input spectra of Table 3, information on how to import them (number of header lines, columns of  $x$ - and  $y$ -values), input and output directories, model constants, model parameter settings (default values, user values of forward and inverse mode, range), settings concerning program operation in the different modes, wavelength range, spectral sampling interval, and visualization.

WASI.INI is automatically read during program start. An update is created either manually during program operation, when the user decides to store the complete set of actual settings, or automatically at program termination (optional). Whenever WASI creates output files, an updated copy of WASI.INI is automatically stored in the relevant directory. Thus, WASI.INI serves as the file which completely documents all calculation settings.

WASI.INI is furthermore the key for other programs to use WASI as a slave that generates or analyzes data according to their inputs. For that, the master program has to modify a copy of WASI.INI and it has to start WASI using the syntax 'WASI <INI-file>', where <INI-file> is a copy of WASI.INI containing the actual settings. When WASI is started in this way, no user interface is opened (background mode), and it automatically performs the sequence of reading <INI-file>, starting calculation as defined in that file, saving the results, and terminating.

## 2.3. User interface

A representative screen shot of WASI's graphical user interface (GUI) is shown in Fig. 1. Some details depend on the mode of operation and on the spectrum type. The GUI consists of eight elements:

1. Drop-down list for selecting the spectrum type.
2. Check boxes for specifying the operation mode. The box "invert spectra" selects between forward and inverse mode. A hook in the "batch mode" check box indicates that a series of spectra is analyzed; otherwise, a single spectrum is inverted (single spectrum mode). The check box "read from file" selects whether the spectra are read from files (hook), or if previously forward calculated spectra are taken (reconstruction mode, no hook).
3. Parameter list. This is the interface for the user to specify parameter settings. All parameters relevant for the selected spectrum type are tabulated. It displays the parameters' symbols (in WASI notation, see Table 2), their values, and, in the inverse mode, a check box for selecting whether a parameter is fitted (hook) or kept constant during inversion (no hook).

Table 2  
Parameter list

Symbol	WASI	Units	Description
$C_i$	C[i]	$\mu\text{g l}^{-1}$	Concentration of phytoplankton class No. $i$ , $i=0\dots5$
$C_L$	C.L	$\text{mg l}^{-1}$	Concentration of large suspended particles
$C_S$	C.S	$\text{mg l}^{-1}$	Concentration of small suspended particles
$X$	C.X	$\text{m}^{-1}$	Concentration of non-chlorophyllous particles
$Y$	C.Y	$\text{m}^{-1}$	Concentration of Gelbstoff
$S$	S	$\text{nm}^{-1}$	Exponent of Gelbstoff absorption
$n$	$n$	—	Exponent of backscattering by small particles
$T$	T.W	$^{\circ}\text{C}$	Water temperature
$f$	$f$	—	Proportionality factor of reflectance (“ $f$ -factor”)
$Q$	$Q$	sr	Anisotropy factor (“ $Q$ -factor”)
$\theta_{\text{sun}}$	Sun	$^{\circ}$	Sun zenith angle
$\theta_v$	View	$^{\circ}$	Viewing angle (0=nadir)
$\sigma_L$	Sigma.L	—	Reflection factor of sky radiance
$\nu$	Nue	—	Exponent of aerosol scattering
$\alpha$	Alpha	—	Fraction of irradiance due to direct solar radiation
$\beta$	Beta	—	Fraction of irradiance due to molecule scattering
$\gamma$	Gamma	—	Fraction of irradiance due to aerosol scattering
$\delta$	Delta	—	Fraction of irradiance due to cloud scattering
$\alpha^*$	Alpha.s	$\text{sr}^{-1}$	Fraction of radiance due to direct solar radiation
$\beta^*$	Beta.s	$\text{sr}^{-1}$	Fraction of radiance due to molecule scattering
$\gamma^*$	Gamma.s	$\text{sr}^{-1}$	Fraction of radiance due to aerosol scattering
$\delta^*$	Delta.s	$\text{sr}^{-1}$	Fraction of radiance due to cloud scattering
$f_n$	fA[n]	—	Areal fraction of bottom surface type no. $n$ , $n=0\dots5$

Table 3  
Input spectra

Symbol	WASI	Units	Description
$\lambda$	$x$	nm	Wavelengths for which spectra are calculated
$a_i^*(\lambda)$	aP[i]	$\text{m}^2 \text{mg}^{-1}$	Specific absorption of phytoplankton class No. $i$ , $i=0\dots5$
$a_X^*(\lambda)$	aX	—	Normalized absorption of non-chlorophyllous particles
$a_Y^*(\lambda)$	aY	—	Normalized absorption of Gelbstoff
$a_W(\lambda)$	aW	$\text{m}^{-1}$	Absorption of pure water
$da_W(\lambda)/dT$	dadT	$\text{m}^{-1} \text{ } ^{\circ}\text{C}^{-1}$	Temperature gradient of pure water absorption
$b_L(\lambda)$	bL	—	Normalized scattering of large suspended particles
$L_s(\lambda)$	Ls	$\text{mW m}^{-2} \text{ nm}^{-1} \text{ sr}^{-1}$	Sky radiance
$E_d(\lambda)$	Ed	$\text{mW m}^{-2} \text{ nm}^{-1}$	Downwelling irradiance above water surface
$R(\lambda)$	R	—	Irradiance reflectance
$a_n(\lambda)$	albedo[n]	—	Albedo of bottom surface type no. $n$ , $n=0\dots5$
$E_0(\lambda)$	E0	$\text{mW m}^{-2} \text{ nm}^{-1}$	Extraterrestrial solar irradiance
$t_A(\lambda)$	tA	—	Transmission of the atmosphere for direct radiation
$t_C(\lambda)$	tC	—	Transmission of clouds
$g_i$	gew	—	Weights of channels at calculation of residuals

Which values are displayed depends on the mode of operation: the actual values are shown in the forward mode, the start values in the inverse mode, and the fit results in the single spectrum mode of inversion.

- The appearance of this area depends on the mode of operation. In the forward and reconstruction mode, a selection panel for specifying the iterations is displayed (see Fig. 2). In the single spectrum mode of inversion, the residuum and the number of

iterations are shown here after calculation is finished. In the batch mode of inversion, this area is empty.

- Check boxes for selecting model options. Several spectrum types support options which further specify the model, cf. Table 1. Each option is either switched on or off.
- Menu bar. Further details concerning the model, data storage and visualization can be specified in various pop-up windows, which are accessed via the menu bar.

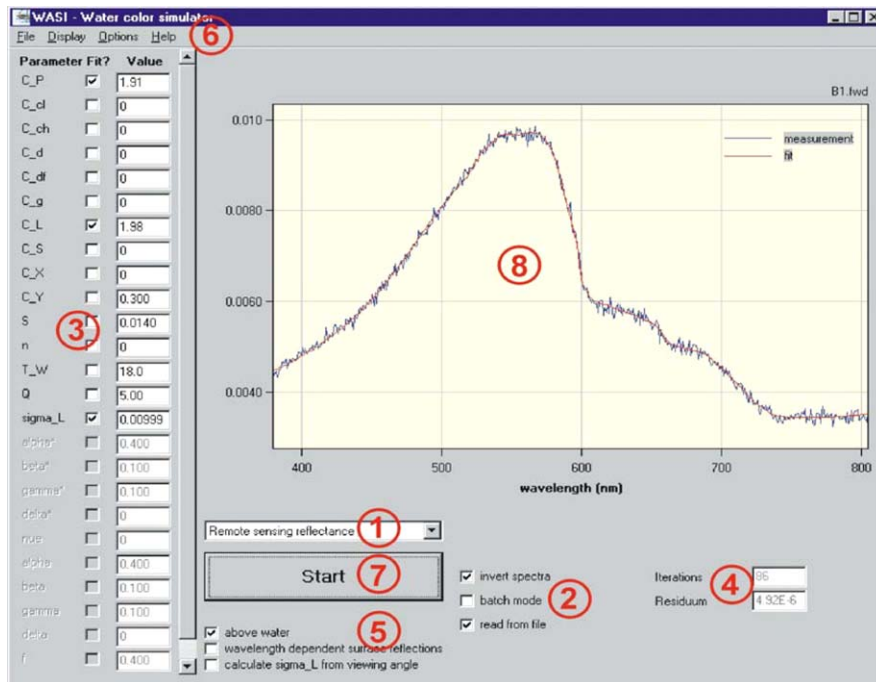


Fig. 1. Graphical user interface of WASI in inverse mode: 1—drop-down list for selecting the spectrum type, 2—check boxes for specifying operation mode, 3—parameter list (model specific), 4—display elements depending on mode of operation, 5—check boxes for selecting model options (model specific), 6—menu bar, 7—start button, and 8—plot window.

7. Start button. Calculation is started by pressing this button.
8. Plot window. For visualization of imported and calculated spectra. All input spectra of Table 3 can be visualized. Calculated spectra are plotted automatically.

In the example of Fig. 1, a remote sensing reflectance spectrum above water, imported from the file B1.fwd, was inverted in the single spectrum mode. The spectrum had been previously generated in the forward mode, where noise with a standard deviation of  $10^{-4} \text{sr}^{-1}$  was added. During inversion three parameters were fitted (C\_P, C\_L, sigma\_L), the other parameters were kept constant. Fit results are  $C_P = 1.91 \mu\text{g l}^{-1}$ ,  $C_L = 1.98 \text{mg l}^{-1}$ , and  $\text{sigma}_L = 0.00999$ . The fit converged after 86 iterations at a residuum of  $4.92 \times 10^{-6} \text{sr}^{-1}$ .

### 3. Models

#### 3.1. Absorption

##### 3.1.1. Water constituents

Absorption of a mixture of water constituents is the sum of the components' absorption:

$$a_{\text{WC}}(\lambda) = \sum_{i=0}^5 C_i a_i^*(\lambda) + X a_X^*(\lambda) + Y a_Y^*(\lambda). \quad (1)$$

$\lambda$  denotes wavelength. Three groups of absorbing water constituents are considered: phytoplankton, non-chlorophyllous particles, and Gelbstoff.

*Phytoplankton*: The high number of species that occur in natural waters causes some variability of the phytoplankton's absorption properties. This is accounted for by the inclusion of six specific absorption spectra  $a_i^*(\lambda)$ . The default spectra provided with WASI are taken from Gege (1998b). The "optical class" number 0 represents a mixture of various phytoplankton species which can be considered typical for Lake Constance. Thus, if no phytoplankton classification is performed, the spectrum  $a_0^*(\lambda)$  is selected to represent the specific absorption of phytoplankton. The  $C_i$  are the pigment concentrations, where "pigment" is the sum of chlorophyll-*a* and phaeophytin-*a*.

*Non-chlorophyllous particles*: Absorption is calculated as product of concentration  $X$  and specific absorption  $a_X^*(\lambda)$ . The spectrum  $a_X^*(\lambda)$  provided with WASI is taken from Prieur and Sathyendranath (1981). It is normalized to 1 at a reference wavelength  $\lambda_0$ .

*Gelbstoff (dissolved organic matter)*: Gelbstoff absorption is the product of concentration  $Y$  and specific absorption  $a_Y^*(\lambda)$ . The spectrum  $a_Y^*(\lambda)$  can either be read from file or calculated using the usual exponential approximation (Nyquist, 1979; Bricaud et al., 1981):

$$a_Y^*(\lambda) = \exp[-S(\lambda - \lambda_0)], \quad (2)$$

where  $S$  denotes the spectral slope, and  $\lambda_0$  is a reference wavelength where  $a_Y^*$  is normalized to 1. Default values are  $\lambda_0 = 440$  nm and  $S = 0.014$  nm<sup>-1</sup>, which can be considered representative of a great variety of water types (Bricaud et al., 1981; Carder et al., 1989).

### 3.1.2. Natural water

The bulk absorption of a natural water body is the sum of absorption of pure water and of the water constituents:

$$a(\lambda) = a_W(\lambda) + (T - T_0) \frac{da_W(\lambda)}{dT} + a_{WC}(\lambda). \quad (3)$$

Absorption of pure water is split up into a temperature-independent term  $a_W$ , which is valid for a reference temperature  $T_0$ , and a temperature gradient  $da_W/dT$  with  $T$  being the actual water temperature. For  $a_W(\lambda)$  the spectrum measured by Buiteveld et al. (1994) at  $T_0 = 20^\circ\text{C}$  is used for 391–787 nm, for  $da_W(\lambda)/dT$  a spectrum is provided which was measured by the author (unpublished data).

### 3.2. Backscattering

Backscattering  $b_b$  of a water body is the sum of backscattering by pure water and suspended particles. In WASI the following parameterization is chosen:

$$b_b(\lambda) = b_{b,W}(\lambda) + C_L b_{b,L}^* b_L(\lambda) + C_S b_{b,S}^* (\lambda/\lambda_S)^n. \quad (4)$$

For pure water, the empirical relation of Morel (1974) is used:  $b_{b,W}(\lambda) = b_1(\lambda/\lambda_1)^{-4.32}$ . The specific backscattering coefficient,  $b_1$ , depends on salinity. It is  $b_1 = 0.00111$  m<sup>-1</sup> for fresh water and  $b_1 = 0.00144$  m<sup>-1</sup> for oceanic water with a salinity of 35–38‰, when  $\lambda_1 = 500$  nm is chosen as reference wavelength.

For suspended matter, a distinction between large ( $\geq 5$  μm, index “L”) and small ( $\leq 5$  μm, index “S”) particles is made. The backscattering of large particles is calculated as the product of concentration  $C_L$ , specific backscattering coefficient  $b_{b,L}^*$ , and normalized scattering function  $b_L(\lambda)$ . The user has several options for calculation:

- $C_L$  can be treated either as an independent parameter, or  $C_L = C_0$  can be set, where  $C_0$  is the concentration of phytoplankton class No. 0 (see Section 3.1.1). The latter is useful for Case 1 water types where the concentrations of particles and phytoplankton are highly correlated.
- $b_{b,L}^*$  can be treated either as constant with a default value of  $0.0086$  m<sup>2</sup> g<sup>-1</sup> (Heege, 2000), or as  $b_{b,L}^* = AC_L^B$ . Such a non-linear dependency of scattering on concentration was observed for phytoplankton (Morel, 1980). It may be used for Case 1 water types, while  $b_{b,L}^* = \text{constant}$  is appropriate for Case 2 waters with significant sources of non-phytoplankton suspended matter. Typical values of the empirical

constants are  $A = 0.0006$  m<sup>2</sup> g<sup>-1</sup> and  $B = -0.37$  (Sathyendranath et al., 1989).

- $b_L(\lambda)$  can either be read from file, or it can be calculated as  $b_L(\lambda) = a_0^*(\lambda_L)/a_0^*(\lambda)$ , where  $a_0^*(\lambda)$  is the specific absorption spectrum of phytoplankton class No. 0 (see Section 3.1.1), and  $\lambda_L$  denotes a reference wavelength. This method assumes that backscattering by large particles originates mainly from phytoplankton cells, and couples absorption and scattering according to Case 1 waters model of Sathyendranath et al. (1989). However, such coupling may be used in exceptional cases only, since living algae have a negligible influence on the backscattering process by oceanic waters (Ahn et al., 1992), and in Case 2 waters particle scattering is related to phytoplankton absorption only weakly in general. In WASI,  $b_L(\lambda) = 1$  is set as default.

Backscattering by small particles is calculated as the product of concentration  $C_S$ , specific backscattering coefficient  $b_{b,S}^*$  and a normalized scattering function  $(\lambda/\lambda_S)^n$ . The exponent  $n$  depends on particle size distribution and is typically in the order of  $-1$  (Sathyendranath et al., 1989).  $b_{b,S}^*$  in the order of  $0.005$  m<sup>2</sup> g<sup>-1</sup> for  $\lambda_S = 500$  nm.

### 3.3. Attenuation

The diffuse attenuation coefficient of downwelling irradiance ( $E_d^-$ ) is defined as  $K_d = -(1/E_d^-) dE_d^-/dz$ , where  $z$  is the depth. It depends not only on the properties of the medium, but also on the geometric structure of the light field. The following parameterization of  $K_d$  is adapted from Gordon (1989), which eliminates the light field effect near the surface to a large extent:

$$K_d(\lambda) = \kappa_0 \frac{a(\lambda) + b_b(\lambda)}{\cos \theta'_{\text{sun}}}. \quad (5)$$

$a(\lambda)$  is calculated according to Eq. (3),  $b_b(\lambda)$  using Eq. (4). The coefficient  $\kappa_0$  depends on the scattering phase function. Gordon (1989) determined a value of  $\kappa_0 = 1.0395$  from Monte Carlo simulations in Case 1 waters, Albert and Mobley (2003) found a value of  $\kappa_0 = 1.0546$  from Hydrolight simulations in Case 2 waters. Some authors use Eq. (5) with  $\kappa_0 = 1$  (Sathyendranath and Platt, 1988, 1997; Gordon et al., 1975). In WASI,  $\kappa_0$  is read from the WASI.INI file; the default value is 1.0546.

### 3.4. Specular reflectance

An above-water radiance sensor looking down to the water surface measures the sum of two radiance components: one from the water body, one from the

surface. The radiance reflected from the surface,  $L_r(\lambda)$ , is a fraction  $\sigma_L$  of sky radiance  $L_s(\lambda)$ :

$$L_r(\lambda) = \sigma_L L_s(\lambda). \quad (6)$$

$L_s(\lambda)$  is the average radiance of that area of the sky that is specularly reflected into the sensor. It can be imported from file or calculated using Eq. (17).  $\sigma_L$  is the Fresnel reflectance and depends on the angle of reflection. The value can either be specified by the user or it can be calculated from the viewing angle  $\theta_v$  using the Fresnel equation for unpolarized light (Jerlov, 1976):

$$\sigma_L = \frac{1}{2} \left| \frac{\sin^2(\theta_v - \theta'_v)}{\sin^2(\theta_v + \theta'_v)} + \frac{\tan^2(\theta_v - \theta'_v)}{\tan^2(\theta_v + \theta'_v)} \right|. \quad (7)$$

$\theta'_v$  is the angle of refraction, which is related to  $\theta_v$  by Snell's law  $n_W \sin \theta'_v = \sin \theta_v$ , where  $n_W \approx 1.33$  is the refractive index of water. For viewing angles near nadir,  $\sigma_L \approx 0.02$ .

The ratio of the radiance reflected from the water surface to the downwelling irradiance,

$$R_{rs}^{surf}(\lambda) = \frac{L_r(\lambda)}{E_d(\lambda)} = \sigma_L \frac{L_s(\lambda)}{E_d(\lambda)}, \quad (8a)$$

is called specular reflectance.  $E_d(\lambda)$  and  $L_s(\lambda)$  can either be imported from file, or one or both can be calculated using Eq. (15) or (17). If the wavelength-independent model of surface reflection is chosen, it is

$$R_{rs}^{surf} = \frac{\sigma_L}{\pi}. \quad (8b)$$

Toole et al. (2000) showed that  $R_{rs}^{surf}(\lambda)$  is nearly spectrally flat at overcast sky, but clearly not for clear-sky conditions. Thus, Eq. (8a) should be used in general, and Eq. (8b) at most for days with overcast sky.

### 3.5. Irradiance reflectance

The ratio of upwelling irradiance to downwelling irradiance in water,  $R(\lambda) = E_u^-(\lambda)/E_d^-(\lambda)$ , is called irradiance reflectance (Mobley, 1994). A suitable parameterization in terms of absorption  $a(\lambda)$  and back-scattering  $b_b(\lambda)$  was found by Gordon et al. (1975):

$$R(\lambda) = f \frac{b_b(\lambda)}{a(\lambda) + b_b(\lambda)}. \quad (9)$$

Independently, Prieur (1976) found the relation  $R(\lambda) = f' b_b(\lambda)/a(\lambda)$ . Both relations are implemented in WASI. The Gordon algorithm (9) is set as default, because it restricts the  $R/f$  values to the physically reasonable range from 0 to 1, which is not the case for the Prieur equation.

The factor  $f$  depends on the scattering properties of the water and on the geometric structure of the light field. It can be treated either as an independent parameter with a default value of 0.33, or the

relationship of Albert and Mobley (2003) can be used:

$$f = 0.1034(1 + 3.3586\omega_b - 6.5358\omega_b^2 + 4.6638\omega_b^3) \left( 1 + \frac{2.4121}{\cos \theta'_{sun}} \right), \quad (10)$$

where  $\omega_b = b_b/(a + b_b)$  and  $\theta'_{sun}$  is the sun zenith angle in water. Also parameterizations of Kirk (1984), Morel and Gentili (1991), and Sathyendranath and Platt (1997) are implemented in WASI and can be selected.

### 3.6. Remote sensing reflectance

The ratio of upwelling radiance to downwelling irradiance,  $R_{rs}(\lambda) = L_u(\lambda)/E_d(\lambda)$ , is called remote sensing reflectance (Mobley, 1994). In water, it is proportional to  $R(\lambda)$ :

$$R_{rs}^-(\lambda) = \frac{R(\lambda)}{Q}. \quad (11)$$

The factor of proportionality,  $Q = E_u^-/L_u^-$ , is a measure for the anisotropy of the upwelling light field and typically in the order of 5 sr. It is treated as a wavelength-independent parameter. Alternately to Eq. (11), the equation  $R_{rs}^-(\lambda) = f_{rs}\omega_b(\lambda)$  can be selected, where  $f_{rs} = f/Q$  is parameterized similarly to Eq. (10) as a function of  $\omega_b$ ,  $\theta'_{sun}$ , and the viewing angle in water,  $\theta'_v$  (Albert and Mobley, 2003).

In air, the remote sensing reflectance is related to  $R(\lambda)$  as follows (Mobley, 1994):

$$R_{rs}(\lambda) = \frac{(1 - \sigma)(1 - \sigma_L^-)}{n_w^2 Q} \frac{R(\lambda)}{1 - \sigma^- R(\lambda)} + R_{rs}^{surf}(\lambda). \quad (12)$$

The first term describes reflection in the water, the second at the surface. Frequently, the first term alone is called remote sensing reflectance (e.g. Mobley, 1994). In WASI, the reflection at the surface is also included in the  $R_{rs}$  definition. It is calculated using Eq. (8a) or (8b) and can easily be excluded by setting  $\sigma_L$  equal to zero.

Two alternate equations for calculating  $R_{rs}(\lambda)$  are also implemented in WASI. The first links remote sensing in water to that in air: in numerator and denominator of Eq. (12)  $R(\lambda)$  is replaced by  $QR_{rs}^-(\lambda)$ . The second avoids the use of the factor  $Q$ , which is difficult to assess: in the numerator  $R(\lambda)$  is replaced by  $QR_{rs}^-(\lambda)$ .

The factors  $\sigma_L^-$ ,  $\sigma$ , and  $\sigma^-$  are the reflection factors for  $L_u^-$ ,  $E_d$ , and  $E_u^-$ , respectively.  $\sigma_L^-$  can either be calculated as a function of  $\theta_v$  using Eq. (7), or a constant value can be taken.  $\sigma$  depends on the radiance distribution and on surface waves. Typical values are 0.02–0.03 for clear sky conditions and solar zenith angles below 45°, and 0.05–0.07 for overcast skies (Jerlov, 1976; Preisendorfer and Mobley, 1985, 1986).  $\sigma^-$  is in the range of 0.50–0.57 with a value of 0.54 being typical (Jerome et al., 1990; Mobley, 1999). Default values are  $\sigma = 0.03$ ,  $\sigma_L^- = 0.02$ ,  $\sigma^- = 0.54$ ,  $Q = 5$  sr, and  $n_w = 1.33$ .

### 3.7. Bottom reflectance

The irradiance reflectance of a surface is called albedo. When  $N$  different surfaces of albedo  $a_n(\lambda)$  are viewed simultaneously, the measured albedo is the following sum:

$$R^b(\lambda) = \sum_{n=0}^{N-1} f_n a_n(\lambda). \quad (13)$$

$f_n$  is the areal fraction of surface number  $n$  within the sensor's field of view; it is  $\sum f_n = 1$ . This equation is implemented in WASI for  $N = 6$  bottom types.

When the upwelling radiation is measured by a radiance sensor, the corresponding remote sensing reflectance can be expressed as follows:

$$R_{rs}^b(\lambda) = \sum_{n=0}^{N-1} f_n B_n a_n(\lambda). \quad (14)$$

$B_n$  is the proportion of radiation which is reflected into the direction of the sensor. In WASI, the  $B_n$ 's of all surfaces are assumed to be angle-independent. The default values are set to  $B_n = 1/\pi = 0.318 \text{ sr}^{-1}$ , which represents isotropic reflection (Lambertian surfaces).

### 3.8. Downwelling irradiance

An analytic model of the downwelling irradiance spectrum  $E_d(\lambda)$  with only few parameters was developed by Gege (1994, 1995). It fits to measured spectra with a high degree of accuracy (average rms error of 0.1%). The radiation illuminating the water surface is parameterized as the sum of four spectrally different components: (1) the direct solar radiation transmitted through the atmosphere, (2) the blue sky, (3) radiation scattered by aerosols, and (4) clouds. Each component is expressed in terms of a wavelength-dependent fraction of the extraterrestrial solar irradiance  $E_0(\lambda)$ :

$$E_d(\lambda) = [\alpha t_A(\lambda) + \beta(\lambda/\lambda_R)^{-4.09} + \gamma(\lambda/\lambda_M)^v + \delta t_C(\lambda)] E_0(\lambda). \quad (15)$$

The four functions  $t_i(\lambda) = \{t_A(\lambda), (\lambda/\lambda_R)^{-4.09}, (\lambda/\lambda_M)^v, t_C(\lambda)\}$  are transmission spectra which spectrally characterize the four light sources. Their weights  $\alpha, \beta, \gamma, \delta$  may change from one measurement to the next, but the  $t_i(\lambda)$  themselves are assumed to be constant. Each  $t_i(\lambda)$  is normalized as  $\int t_i(\lambda) E_0(\lambda) d\lambda = \int E_0(\lambda) d\lambda$ ; the integration interval is set to 400–800 nm by default.

The functions  $(\lambda/\lambda_R)^{-4.09}$  and  $(\lambda/\lambda_M)^v$  are calculated during run-time. Normalization yields their scaling factors:  $\lambda_R = 533 \text{ nm}$ , and  $\lambda_M$  is typically between 563 nm ( $v = -1$ ) and 583 nm ( $v = 1$ ). The exponent  $v$  parameterizes the wavelength dependency of aerosol scattering. The two other functions,  $t_A(\lambda)$  and  $t_C(\lambda)$ , are read from file. After import they are normalized. The

two provided with WASI were determined from measurements at Lake Constance.

The downwelling irradiance in water,  $E_d^-$ , is related to the downwelling irradiance in air,  $E_d$ , through  $E_d^-(\lambda) = (1 - \sigma)E_d(\lambda) + \sigma^- E_u^-(\lambda)$ .  $\sigma$  is the reflection factor for downwelling irradiance in air,  $\sigma^-$  for upwelling irradiance in water, and  $E_u^-$  is the upwelling irradiance in water. Using the irradiance reflectance  $R = E_u^-/E_d^-$  yields the following expression:

$$E_d^-(\lambda) = \frac{1 - \sigma}{1 - \sigma^- R(\lambda)} E_d(\lambda). \quad (16)$$

This equation is used in WASI for calculating  $E_d^-(\lambda)$ .  $R(\lambda)$  is calculated using Eq. (9).  $E_d(\lambda)$  can either be calculated according to Eq. (15), or a measured spectrum can be taken. Default values of the reflection factors are  $\sigma = 0.03$  and  $\sigma^- = 0.54$ .

### 3.9. Sky radiance

The same parameterization as for  $E_d(\lambda)$  is also implemented for  $L_s(\lambda)$ :

$$L_s(\lambda) = [\alpha^* t_A(\lambda) + \beta^*(\lambda/\lambda_R)^{-4.09} + \gamma^*(\lambda/\lambda_M)^v + \delta^* t_C(\lambda)] E_0(\lambda). \quad (17)$$

The functions  $E_0(\lambda)$ ,  $t_A(\lambda)$ ,  $(\lambda/\lambda_R)^{-4.09}$ ,  $(\lambda/\lambda_M)^v$ , and  $t_C(\lambda)$  are those of Eq. (15). Parameters of  $L_s(\lambda)$  are the weights  $\alpha^*, \beta^*, \gamma^*, \delta^*$ , which represent the relative intensities of the four above-mentioned light sources for a radiance sensor, and the exponent  $v$ .

This model of  $L_s(\lambda)$  has been included for modeling specular reflection at the water surface. Its usefulness has been demonstrated (Gege, 1998a). Capillary waves at the water surface, and moreover gravity waves, spread greatly the sky area that is reflected into a radiance sensor, and change the angle of reflection. Consequently, measurements of  $L_s(\lambda)$  are frequently not representative. For these cases, and if no  $L_s(\lambda)$  measurement is available, Eq. (17) can be applied. If the wavelength-independent model of surface reflection is chosen,  $L_s(\lambda) = E_d(\lambda)/\pi$  is set.

### 3.10. Upwelling radiance

The upwelling radiance is that part of the downwelling irradiance which is reflected back from the water into a down-looking radiance sensor. Calculation is based on a model of  $R_{rs}$  and a model or a measurement of  $E_d$ .

In water, Eq. (16) is used for calculating  $E_d^-(\lambda)$ , and Eq. (11) for  $R_{rs}^-(\lambda)$ . The upwelling radiance is then calculated as follows:

$$L_u^-(\lambda) = R_{rs}^-(\lambda) E_d^-(\lambda). \quad (18)$$

In air, the upwelling radiance after crossing the water-air boundary is related to  $L_u^-$  as follows:

$$L_u(\lambda) = \frac{1 - \sigma_L^-}{n_w^2} L_u^-(\lambda) + L_r(\lambda). \quad (19)$$

The first term on the right-hand side is the radiance upwelling in the water, weakened at the interface by Fresnel reflection (factor  $1 - \sigma_L^-$ ) and refraction (flux dilution by widening of the solid angle, factor  $1/n_w^2$ ).  $L_u^-(\lambda)$  is obtained from Eq. (18),  $L_r(\lambda)$  from Eq. (6).  $\sigma_L^-$  can either be calculated as a function of  $\theta_v$  using Eq. (7), or a constant value can be taken. Default values of the constants are  $\sigma_L^- = 0.02$  and  $n_w = 1.33$ .

#### 4. Forward modeling

Forward modeling is the calculation of spectra according to user-specified parameter settings. During a run, either a single spectrum or a series of spectra is calculated. For calculating a series of spectra, up to three parameters from Table 2 can be iterated simultaneously. The iterated parameters, their range of variation, and the number of steps are specified using the selection panel shown in Fig. 2. In the forward mode, this panel is always displayed in the main window (as element number 4 of Fig. 1). The check boxes labeled “log” specify whether the parameter intervals are equidistant on a linear scale (no hook) or on a logarithmic scale (hook).

The calculated spectra are automatically plotted on screen, and can be saved as individual files in ASCII format. Two features are implemented which are useful for performing sensor-specific simulations:

- Gaussian distributed noise can be added. The user has to specify the standard deviation.
- The radiometric dynamics can be reduced. This is realised by user-specified rounding of calculated spectral values.

Parameter	from	to	steps	log
C[0]	0.100	10.0	7	<input checked="" type="checkbox"/>
C_Y	0.100	1	4	<input type="checkbox"/>
none	0.100	1	10	<input type="checkbox"/>

Fig. 2. Selection panel for specifying parameter iteration at forward calculation.

#### 5. Inverse modeling

Inverse modeling is the determination of model parameters for a given spectrum. Table 2 summarizes all parameters whose values can principally be determined via fit. The actual number of fit parameters depends on the spectrum type, on model options, and on the user’s choice which parameters to fit and which to fix during inversion. Three modes of operation are implemented:

- *Single spectrum mode.* Fitting is performed for a single spectrum which the user loads from file. After inversion, an overlay of imported spectrum and fit curve is automatically shown on screen and resulting fit values, number of iterations, and residuum are displayed. This mode allows to inspect the fit results of individual measurements. It is useful for optimizing the choice of initial values and the fit strategy before starting a batch job.
- *Batch mode.* A series of spectra from file is fitted. After each inversion, an overlay of imported spectrum and fit curve is automatically shown on screen. This mode is useful for processing large data sets.
- *Reconstruction mode.* Combines forward and inverse modes. Inversion is performed for a series of forward calculated spectra which are not necessarily read from file. The model parameters can be chosen differently for forward and inverse calculations. This mode is useful for performing sensitivity studies.

The fit parameters are determined iteratively: in the first iteration, a model spectrum is calculated using initial values for the fit parameters. This model spectrum is compared with the measured spectrum by calculating the residuum as a measure of correspondence. Then, in the further iterations, the values of the fit parameters are altered, resulting in altered model curves and altered residuals. For selecting a new set of parameter values from the previous sets, the Simplex algorithm is used (Nelder and Mead, 1965; Caceci and Cacheris, 1984). The procedure is stopped after the best fit between calculated and measured spectrum has been found, which corresponds to the minimum residuum. The values that were used in the step with the smallest residuum are the results.

If the solution of the inversion problem is ambiguous, the inversion algorithm may not find the correct values of the fit parameters. The problem occurs when different sets of model parameters yield similar spectra, i.e. the problem is model specific. Measures are implemented in WASI to handle the ambiguity problem. The most effective measure is to use “realistic” values of all fit parameters as initial values when inversion is started. Methods are implemented to determine automatically

start values of some parameters. Other fit tuning measures are to restrict the search to the expected range, or to weight the spectral information differently for individual spectral channels. The description and discussion of these measures is out of scope of this article. A paper focusing on the inversion subject is in preparation; some details are also described in the manual (Gege, 2002).

## 6. Conclusions

The Water Colour Simulator, WASI, is a software which integrates forward and inverse modeling for eight common types of optical in situ measurements in aquatic environments. It is designed for effectively generating, analyzing, and visualizing series of spectra. Computing is fast: for example, 0.17 s per spectrum were required on average using a 450 MHz Pentium III notebook for determining the concentrations  $C_0$ ,  $C_L$  and  $Y$  from 1331 irradiance reflectance spectra by inverse modeling of 300 channels (Gege, 2003).

The focus of the implemented models is on measurements in deep water. In addition, models for the illumination (downwelling irradiance, sky radiance) and for linear combinations of reflectance spectra (bottom reflectance) are included. Algorithms for shallow water applications have been developed recently (Albert and Mobley, 2003). Their implementation in WASI is in progress. For the future it is planned to account for physical effects which are so far ignored (fluorescence, Raman scattering), and to cope with vertical profiles.

## References

- Ahn, Y.H., Bricaud, A., Morel, A., 1992. Light backscattering efficiency and related properties of some phytoplankton. *Deep-Sea Research* 39 (11/12), 1835–1855.
- Albert, A., Mobley, C.D., 2003. An analytical model for subsurface irradiance and remote sensing reflectance in deep and shallow case-2 waters. *Optics Express* 11 (22), 2873–2890.
- Bricaud, A., Morel, A., Prieur, L., 1981. Absorption by dissolved organic matter of the sea (yellow substance) in the UV and visible domains. *Limnology and Oceanography* 26 (1), 43–53.
- Buiteveld, H., Hakvoort, J.H.M., Donze, M., 1994. The optical properties of pure water. In: *Proceedings Ocean Optics XII*, SPIE, Vol. 2258. pp. 174–183.
- Caccci, M.S., Cachier, W.P., 1984. Fitting curves to data. *Byte* 340–362.
- Carder, K.L., Steward, R.G., Harvey, G.R., Ortner, P.B., 1989. Marine humic and fulvic acids: their effects on remote sensing of ocean chlorophyll. *Limnology and Oceanography* 34 (1), 68–81.
- Gege, P., 1994. *Gewässeranalyse mit passiver Fernerkundung: Ein Modell zur Interpretation optischer Spektralmessungen*. Dissertation, DLR-Forschungsbericht 94-15, 171pp.
- Gege, P., 1995. *Water analysis by remote sensing: a model for the interpretation of optical spectral measurements*. Technical Translation ESA-TT-1324, July 1995, 231pp.
- Gege, P., 1998a. Correction of specular reflections at the water surface. In: *Proceedings Ocean Optics XIV*, 10–13 November 1998, Conference Papers, Vol. 2. Kailua-Kona, Hawaii, USA.
- Gege, P., 1998b. Characterization of the phytoplankton in Lake Constance for classification by remote sensing. In: Bäumler, E., Gaedke, U. (Eds.), *Lake Constance—Characterization of an ecosystem in transition*. *Archiv für Hydrobiologie, special issues: Advances in Limnology* 53, 179–193.
- Gege, P., 2002. *The Water Colour Simulator WASI. User manual for version 2*. DLR Internal Report IB 564-01/02, 60pp.
- Gege, P., 2003. Wasi—a software tool for water spectra. *Backscatter* 14 (1), 22–24.
- Gordon, H.R., 1989. Can the Lambert–Beer law be applied to the diffuse attenuation coefficient of ocean water? *Limnology and Oceanography* 34 (8), 1389–1409.
- Gordon, H.R., Brown, O.B., Jacobs, M.M., 1975. Computed relationships between the inherent and apparent optical properties of a flat homogeneous ocean. *Applied Optics* 14 (2), 417–427.
- Heege, T., 2000. *Flugzeuggestützte Fernerkundung von Wasserinhaltsstoffen im Bodensee*. Dissertation, DLR-Forschungsbericht 2000-40, 141pp.
- Jerlov, N.G., 1976. *Marine Optics*. Elsevier Scientific Publishing Company, Amsterdam, The Netherlands 231pp.
- Jerome, J.H., Bukata, R.P., Bruton, J.E., 1990. Determination of available subsurface light for photochemical and photobiological activity. *Journal of Great Lakes Research* 16 (3), 436–443.
- Kirk, J.T.O., 1984. Dependence of relationship between inherent and apparent optical properties of water on solar altitude. *Limnology and Oceanography* 29 (2), 350–356.
- Mobley, C.D., 1994. *Light and Water*. Academic Press, San Diego 592pp.
- Mobley, C.D., 1999. Estimation of the remote-sensing reflectance from above-surface measurements. *Applied Optics* 38 (36), 7442–7455.
- Morel, A., 1974. Optical properties of pure water and pure sea water. In: Jerlov, N.G., Steemann, N.E. (Eds.), *Optical Aspects of Oceanography*. Academic Press, London, pp. 1–24.
- Morel, A., 1980. In water and remote measurements of ocean colour. *Boundary-Layer Meteorology* 18, 177–201.
- Morel, A., Gentili, B., 1991. Diffuse reflectance of oceanic waters: its dependence on Sun angle as influenced by the molecular scattering contribution. *Applied Optics* 30 (30), 4427–4438.
- Nelder, J.A., Mead, R., 1965. A simplex method for function minimization. *Computer Journal* 7, 308–313.
- Nyquist, G., 1979. Investigation of some optical properties of seawater with special reference to lignin sulfonates and

- humic substances. Dissertation, Göteborgs Universitet, 200pp.
- Preisendorfer, R.W., Mobley, C.D., 1985. Unpolarized irradiance reflectances and glitter patterns of random capillary waves on lakes and seas by Monte Carlo simulation. NOAA Technical Memorandum ERL PMEL-63, Pacific Marine Environment Laboratory, Seattle, WA, 141pp.
- Preisendorfer, R.W., Mobley, C.D., 1986. Albedos and glitter patterns of a wind-roughened sea surface. *Journal of Physical Oceanography* 16 (7), 1293–1316.
- Prieur, L., 1976. Transfers radiatifs dans les eaux de mer. Dissertation, Doctorat d'Etat, Université Pierre et Marie Curie, Paris, 243pp.
- Prieur, L., Sathyendranath, S., 1981. An optical classification of coastal and oceanic waters based on the specific spectral absorption curves of phytoplankton pigments, dissolved organic matter, and other particulate materials. *Limnology and Oceanography* 26 (4), 671–689.
- Sathyendranath, S., Platt, T., 1988. Oceanic primary production: estimation by remote sensing at local and regional scales. *Science* 241, 1613–1620.
- Sathyendranath, S., Platt, T., 1997. Analytic model of ocean color. *Applied Optics* 36 (12), 2620–2629.
- Sathyendranath, S., Prieur, L., Morel, A., 1989. A three-component model of ocean colour and its application to remote sensing of phytoplankton pigments in coastal waters. *International Journal of Remote Sensing* 10 (8), 1373–1394.
- Toole, D.A., Siegel, D.A., Menzies, D.W., Neumann, M.J., Smith, R.C., 2000. Remote-sensing reflectance determinations in the coastal ocean environment: impact of instrumental characteristics and environmental variability. *Applied Optics* 39 (3), 456–469.